Evaluation of *trans*-9-^{18}F-Fluoro-3,4-Methyleneheptadecanoic Acid as a PET Tracer for Myocardial Fatty Acid Imaging

Timothy M. Shoup, PhD; David R. Elmaleh, PhD; Ali A. Bonab, PhD; and Alan J. Fischman, MD, PhD

Division of Nuclear Medicine, Department of Radiology, Massachusetts General Hospital, Boston, Massachusetts

This study describes the radiosynthesis and preliminary biologic evaluation of *trans*-9(*RS*)-^{18}F-fluoro-3,4(*RS*,*RS*)-methyleneheptadecanoic acid (^{18}F-FCPHA) as a new potential probe for assessing myocardial fatty acid metabolism by PET. This fatty acid, containing a cyclopropyl moiety in the β,γ-position, was designed to enter the myocardium by the same mechanism as natural fatty acids and to undergo partial metabolism before being trapped in the cell. **Methods:** ^{18}F-FCPHA and the β-methyl analog 8(*RS*)-^{18}F-fluoro-3(*RS*)-methylheptadecanoic acid (^{18}F-FBMHA) were prepared from their corresponding mesylate precursors by nucleophilic substitution. The precursors used for labeling were fully characterized, and the data were consistent with the proposed structures. Biodistribution studies of each tracer were performed with Sprague–Dawley rats at 5 and 60 min after injection. Sequential imaging of a rhesus monkey injected with 222 MBq of ^{18}F-FCPHA was performed by use of a microPET camera. **Results:** At 5 and 60 min, heart uptake values measured as mean ± SD percentage injected dose per gram (%ID/g) in rats for ^{18}F-FCPHA were 1.55 ± 0.72 and 1.43 ± 0.14, respectively. The heart-to-blood ratios at 5 and 60 min, an indication of target definition, were 25.8 and 20.4, respectively. The heart-to-lung ratios at 5 and 60 min were 3.3 and 4.6, respectively. Bone accumulation (%ID/g), an indication of defluorination, was 0.16 ± 0.03 at 5 min and increased to 0.70 ± 0.39 at 60 min. The heart-to-blood ratio obtained with ^{18}F-FBMHA was 2.6 at 5 min and did not change significantly at 60 min. Imaging of the monkey heart after injection of ^{18}F-FCPHA showed an initial spike of activity corresponding to blood flow followed by a plateau at 10 min. **Conclusion:** The cyclopropyl moiety in ^{18}F-FCPHA does have a significant influence on heart accumulation, as suggested by the high heart-to-blood ratio and the fast blood clearance in rats. These results, along with the remarkable quality of the PET images, indicate the potential of this new class of labeled fatty acids for use in studying heart disease by PET.

Key Words: ^{18}F fatty acid; PET; myocardial fatty acid imaging

J Nucl Med 2005; 46:297–304

Radionuclide imaging of myocardial perfusion and ventricular function is useful for identifying areas of ischemia and defining its impact on global and regional functions. Myocardial flow can be assessed by PET with ^{13}N-ammonia or ^{82}Rb or by SPECT with ^{201}Tl or ^{99m}Tc-sestamibi. Although measurements with these agents usually provide complementary data in patients with stable coronary artery disease, situations in which the information is inconsistent occur (*1,2*). Perfusion and function are discordant immediately after thrombolysis (*3,4*) and in some patients with cardiomyopathy (*5,6*). Both circumstances may result in markedly depressed function when regional perfusion is near normal. These observations suggest that in addition to perfusion and function, other simultaneous measurements, such as substrate metabolism, are needed to better characterize the metabolic viability of the injured myocardium.

Myocardial metabolism is most often assessed with 2-^{18}F-FDG (^{18}F-FDG), a glucose analog that is carried into the cell by a specific glucose membrane transporter and phosphorylated by hexokinase. This agent permits the detection of exogenous glucose utilization in areas of decreased perfusion, indicating the presence of an ischemic myocardium that has preferentially shifted its metabolic substrate toward glucose rather than fatty acids or lactate (*7,8*). Studies have consistently shown the ability of ^{18}F-FDG and PET to identify ischemic myocardium in 10%–20% of regions that otherwise would be classified as infarcted when imaged with ^{201}Tl or ^{99m}Tc-sestamibi (*9,10*). Hence, a mismatch between glucose utilization and perfusion determined by PET is an indication of ischemic but viable myocardium. However, there are concerns with this method because regional myocardial blood flow and ^{18}F-FDG uptake patterns can be similar in various types of myocardial dysfunction (*11–13*).

Another PET metabolic tracer that is used to assess oxidative metabolism and that is deemed to be superior to ^{18}F-FDG is ^{11}C-acetate. Its uptake reflects overall O_2 metabolism by myocytes and does not depend on plasma substrate concentrations or on blood glucose levels, which can influence ^{18}F-FDG distribution. ^{11}C-Acetate imaging is considered more useful than ^{18}F-FDG imaging for assessing

Received Apr. 21, 2004; revision accepted Sep. 13, 2004.

For correspondence or reprints contact: David R. Elmaleh, PhD, Harvard Medical School, Massachusetts General Hospital, Bartlett 508R, Boston, MA 02114.

E-mail: elmaleh@helix.mgh.harvard.edu

postintervention recovery of myocardial function; however, the 20-min half-life of ^{11}C restricts its use to institutions with an on-site cyclotron.

Labeled fatty acids were originally developed to detect myocardial ischemia in which the energy substrate shifts from fatty acids to glucose. Fatty acids are the major source of energy for the myocardium, and their uptake is proportional to blood flow as well as concentration (*14*). Fatty acids are cleared from the blood with a half-life of less than 2 min and are concentrated in the myocardium with a first-pass extraction fraction of 50%–60%. In zones of myocardial ischemia, stunning, and hibernation, fatty acid extraction and oxidation are reduced. Thus, an alteration in fatty acid uptake is considered to be a sensitive marker of ischemia and myocardial damage (*15*).

The use of ^{11}C-palmitate as a physiologic substrate provided the experimental basis for measuring myocardial fatty acid metabolism by PET (*16,17*). After the initial uptake of ^{11}C-palmitate, a rapid loss of radioactivity from myocardial tissue corresponds to straight-chain fatty acid catabolism by β-oxidation. In areas of ischemia or hypoxia, the uptake of the agent and the rate of clearance are diminished, consistent with reduced oxidative metabolism. Unfortunately, in addition to the disadvantage of brief imaging time because of rapid catabolism, ^{11}C-palmitate is also distributed among different tissue pools with variable turnover rates, significantly complicating data analysis (*18*).

1-^{11}C-3-Methylheptadecanoic acid (^{11}C-BMHA) was designed to enter the myocardium by the same mechanism as normal fatty acids; however, because the methyl group inhibits β-oxidation, the tracer is trapped in the cell because of incomplete metabolism (*19,20*). ^{11}C-BMHA was shown to be incorporated into the same lipid pools as ^{11}C-palmitate and to have high retention of activity in the myocardium and excellent imaging properties (*21*). On the basis of these results, several iodinated branched-chain fatty acids were introduced for the purpose of assessing myocardial fatty acid metabolism by SPECT (*15,22,23*). Among these, 15-^{123}I-(*p*-iodophenyl)-3(*RS*)-methylpentadecanoic acid (BMIPP) has been investigated extensively and is an approved radiotracer for clinical use in Japan.

An ^{18}F-labeled fatty acid that is retained in the heart should allow high-resolution PET images that could simplify activity quantitation with an appropriate mathematic model. In this article, we report on the preparation and preliminary evaluation of *trans*-9(*RS*)-^{18}F-fluoro-3,4(*RS*,*RS*)-methyleneheptadecanoic acid (^{18}F-FCPHA; compound 2) as part of a new series of modified fatty acids for myocardial metabolic imaging. ^{18}F-FCPHA contains a cyclopropyl moiety that is present in a wide variety of naturally occurring compounds (*24*). The small size of this moiety allows 2 adjacent carbon sites to inhibit the oxidation process with a minimal change in overall fatty acid structure. Moreover, the cyclopropyl group possesses unique chemical properties attributable to its inherent ring strain and is often an essential staging element in biotransformations.

The biodistribution of ^{18}F-FCPHA was studied in rats and its myocardial extraction and retention were measured in a monkey by use of sequential PET. Finally, the significance of the cyclopropyl moiety on heart uptake was further demonstrated by comparing the biodistribution of the β-methyl analog ^{18}F-8-fluoro-3-methylheptadecanoic acid (^{18}F-FBMHA; compound 4) with that of ^{18}F-FCPHA.

MATERIALS AND METHODS

Chemicals and solvents used in this study were American Chemical Society grade, except for acetonitrile, which was silylation grade (Pierce Chemical Co.), and all were used without additional purification. Compounds 1 and 3 were purified and fully characterized by ^{1}H nuclear magnetic resonance and mass spectrometry analyses (T.M. Shoup, unpublished data, 2004). ^{18}F-Fluoride was produced at Massachusetts General Hospital with a Scanditronix MC-17F cyclotron by the ^{18}O(p,n)^{18}F nuclear reaction on 95% ^{18}O-enriched water in a silver target at 17 MeV and 24 μA per hour. Radio–thin-layer chromatography (radio-TLC) counts were determined with a Bioscan System 200 (Bioscan, Inc.) on 250-μm silica gel AL SILG/UV plates (Whatman Ltd.).

Chemistry

The following labeling procedure was used to prepare compounds 2 and 4 (Scheme 1). A Wheaton 5-mL reaction vial containing ^{18}F (100 mCi) in 0.5 mL of ^{18}O-enriched water, Kryptofix-2.2.2 (8 mg), and potassium carbonate (2 mg) was heated at 118°C, and the solvent was evaporated with the aid of nitrogen gas. The K^{18}F-Kryptofix complex was dried by the addition of 1 mL of acetonitrile followed by evaporation of the solvent by use of nitrogen flow; this step was repeated 3 times. A solution of 8 mg of the mesylate (compound 1 or 3 in Scheme 1) in 1 mL of acetonitrile was added to the vial, and the fluorination reaction was

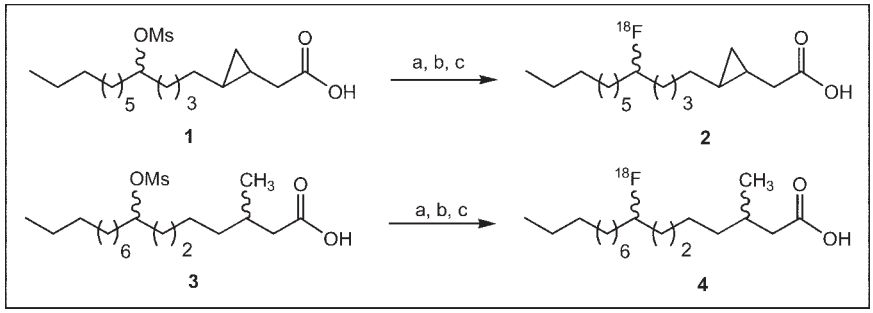

SCHEME 1. Radiosynthesis of ^{18}F-FCPHA (compound 2) and ^{18}F-FBMHA (compound 4). (a) K^{18}F-Kryptofix, acetonitrile, 120°C. (b) Aqueous LiOH (1 mol/L): methanol, 80°C. (c) 10% HCl.

performed at 120°C for 10 min. The solvent was removed by use of nitrogen flow and replaced with 1 mL of a hexane:ethyl acetate (85:15) solution. After the solution was mixed, it was loaded onto a silica gel Sep-Pak (Waters), and the activity was eluted with 3 mL of the same hexane:ethyl acetate solution. The eluent containing the labeled ester was placed in a 5-mL vial, and the solvent was removed. A mixture of 0.5 mL of lithium hydroxide (1 mol/L) and 1 mL of methanol was added to the reaction vial, the vial was heated at 100°C for 20 min, and the reaction volume was reduced to less than 1 mL. The solution was acidified by the addition of 5 mL of 10% HCl, and the mixture was extracted twice with diethyl ether. The ether extracts were combined, and the solvent was removed. The synthesis was complete within 90 min, with an overall yield of final product (compound 2 or 4) of 777 MBq (38% end of bombardment). Radio-TLC revealed 94% radiochemical purity (silica gel plates; ethyl acetate:hexane, 25:75; R_f = 0.40), with the remaining activity as unhydrolyzed ester (silica gel plates; ethyl acetate:hexane, 15:85; R_f = 0.80). The labeled fatty acids were formulated in 10% ethanol in saline for biodistribution in rats and 4% bovine serum albumin in saline for monkey studies (0.22-μm Millex-GV sterile filter; Millipore).

FCPHA and FBMHA were prepared from their corresponding hydroxy esters. The alcohols (100 mg) in methylene chloride (10 mL) were treated with diethylaminosulfur trifluoride (200 μL) at −78°C. The reaction mixtures were stirred at −40°C for 1 h before being quenched with methanol (100 μL) and washed with saturated sodium bicarbonate. Chromatography (silica gel; ethyl acetate:hexane, 5:95) afforded the fluorinated esters, which were converted to the acids by use of LiOH (1 mol/L):methanol (1:3) at reflux for 1 h. The solvent was removed, 10% HCl (10 mL) was added, and the acids were extracted with ether (10 mL; 3 times). Chromatography (silica gel; ethyl acetate:hexane, 20:80) afforded the fluorinated acids in 15% yields. Data were as follows: for FCPHA—^{1}H nuclear magnetic resonance (400 MHz, $CDCl_3$) δ 0.32 (2H, m, ring—CH_2), 0.55 (1H, m, ring—CH), 0.78 (1H, m, ring—CH), 0.89 (3H, t, J = 6 Hz, CH_3), 1.2–1.8 (22H, m, CH_2), 2.25 (2H, d, CH_2—C═O), 4.45 (1H, br-d, J = 53 Hz, FCH); and for FBMHA—δ 0.88 (3H, t, J = 6 Hz, CH_3), 0.92 (3H, d, J = 6 Hz, CH_3), 1.2–1.9 (24H, m, CH_2), 2.25 (2H, dd, CH_2—C═O), 4.46 (1H, br-d, J = 53 Hz, FCH).

Tissue Distribution Studies

The distribution of radioactivity in tissues of male Sprague–Dawley rats (300–350 g; Charles River Breeding Laboratories) was determined after intravenous administration of the radiofluorinated compounds. The animals were allowed food and water ad libitum before the studies. Either ^{18}F-FCPHA or ^{18}F-FBMHA (1.48–2.96 MBq) was injected directly into the tail veins of unanesthetized rats. At 5 and 60 min after injection, groups of 6 animals were sacrificed with an overdose of sodium pentobarbital, and biodistribution was determined. Samples of blood, heart, lungs, liver, kidneys, bone, skeletal muscle, and brain were weighed, and radioactivity was measured with a well-type γ-scintillation counter (model 1282; LKB). To correct for radioactive decay and permit the calculation of radioactivity in each organ as a fraction of the administered dose, counts in aliquots of the injected doses were determined simultaneously. The results were expressed as mean ± SD percentage injected dose per gram (%ID/g).

microPET Measurements

Imaging was performed by use of a microPET model P4 device (Concorde Microsystems). The monkey was positioned supine on the microPET table, injected with 222 MBq of ^{18}F-FCPHA via a femoral line, and imaged for 90 min in list mode. The emission data were binned into 3-dimensional sinograms by use of Fourier rebinning to produce 24 time frames (8 × 15 s, 8 × 60 s, and 8 × 600 s) and were reconstructed by use of a filtered-backprojection algorithm with a ramp filter (Nyquist cutoff at 0.5). A 30-min transmission image was acquired in single mode with a rotating pin source containing ^{68}Ge. The reconstructed data were corrected for scattered radiation, attenuation, and dead time. Regions of interest (ROIs) were drawn over the left ventricular wall, and cardiac blood pool and time–activity curves were constructed.

Statistical Methods

The data were analyzed by 2-way ANOVA with a linear model in which the classification variables were tissue and time: %ID/g = tissue + time + (tissue × time). Post hoc comparisons of individual means were performed with the Student–Newman–Keuls test. All results were expressed as mean ± SD.

RESULTS

Radiochemistry

Radiofluorination of *trans*-9-methanesulfonoxy-3,4-methyleneheptadecanoate methyl ester (compound 1) was achieved by a nucleophilic substitution reaction with the K^{18}F-Kryptofix complex in acetonitrile. After 10 min at 120°C, radio-TLC of the reaction mixture revealed >94% labeled ester, with the remaining activity as ^{18}F-fluoride. Because of the differences in the lipophilicities of the labeled ester (R_f = 0.2) and precursor 1 (R_f = 0.9), purification of the labeled ester was performed with a silica gel Sep-Pak and hexane:ethyl acetate (85:15) for elution of the activity. Base hydrolysis of the ester with lithium hydroxide (1 mol/L) and then acidification produced compound 2 (or compound 4, when starting with compound 3) without detectable defluorination. The synthesis was complete in 90 min, with radiochemical yields of 30%–40% (corrected for decay) (n = 8).

TABLE 1
Tissue Distribution of ^{18}F-FCPHA in Sprague–Dawley Rats

Tissue	Mean ± SD %ID/g at: 5 min	60 min
Blood	0.06 ± 0.01	0.08 ± 0.02
Heart	1.55 ± 0.72	1.43 ± 0.14
Lungs	0.47 ± 0.13	0.31 ± 0.16
Liver	1.34 ± 0.26	0.87 ± 0.15*
Kidneys	0.41 ± 0.10	0.34 ± 0.09
Skeletal muscle	0.25 ± 0.01	0.10 ± 0.01†
Bone	0.16 ± 0.03	0.70 ± 0.39*
Brain	0.06 ± 0.01	0.05 ± 0.02

*$P < 0.05$.
†$P < 0.01$.

Biodistribution

Table 1 shows the biodistribution of ^{18}F-FCPHA at 5 and 60 min after intravenous administration in rats. ANOVA demonstrated a highly significant main effect of tissue ($F_{7,80} = 65.88$; $P < 0.0001$) and a significant interaction of tissue and time ($F_{7,80} = 6.29$; $P < 0.0001$). The main effect of time was not significant ($F_{1,80} = 1.63$; $P = 0.21$). At 5 min, the accumulation of ^{18}F-FCPHA in the heart and liver was significantly greater ($P < 0.01$) than that in any of the other tissues sampled. At 60 min, the accumulation of ^{18}F-FCPHA in the heart was significantly greater ($P < 0.01$) than that in the kidneys, lungs, skeletal muscle, blood, and brain. The accumulation in the liver was significantly greater ($P < 0.05$) than that in the kidneys, lungs, skeletal muscle, blood, and brain, whereas the accumulation in the bone, kidneys, and lungs was significantly greater ($P < 0.01$) than that in the skeletal muscle, blood, and brain.

At 5 min, the accumulation of ^{18}F-FCPHA in the heart (1.55 ± 0.72 %ID/g) was 25.8 times higher than that in the blood. At 60 min, the uptake of radioactivity in the heart decreased slightly to 1.43 ± 0.14 %ID/g (P = NS), to yield a heart-to-blood ratio of 20.4 (Table 2). Blood activity did not change sufficiently from 5 to 60 min. Lung activity was 0.47 ± 0.13 %ID/g at 5 min and decreased to 0.31 ± 0.16 %ID/g at 60 min (P = NS), liver uptake was 1.34 ± 0.26 %ID/g at 5 min and decreased to 0.87 ± 0.15 %ID/g at 60 min ($P < 0.05$), and skeletal muscle uptake was 0.25 ± 0.01 %ID/g at 5 min and decreased to 0.10 ± 0.01 %ID/g at 60 min. Heart-to-lung ratios at 5 and 60 min were 3.3 and 4.6, respectively (Table 2). Tracer accumulation in bone, an indication of defluorination, was 0.16 ± 0.03 %ID/g at 5 min and increased to 0.70 ± 0.39 %ID/g at 60 min ($P < 0.05$).

The biodistribution of the β-methyl analog ^{18}F-FBMHA at 5 and 60 min after intravenous administration in rats is shown in Table 3. ANOVA demonstrated a highly significant main effect of tissue ($F_{7,80} = 89.74$; $P < 0.0001$), a significant main effect of time ($F_{1,80} = 8.90$; $P < 0.005$), and a highly significant interaction of tissue and time ($F_{7,80} = 13.77$; $P < 0.0001$). At 5 min, the accumulation of ^{18}F-FBMHA in the liver was significantly greater ($P < 0.01$) than that in any of the other tissues sampled. The accumulation in the kidneys was significantly greater ($P < 0.01$) than that in the lungs, blood, skeletal muscle, and bone. The accumulation in the heart was significantly greater ($P < 0.01$) than that in the lungs, blood, skeletal muscle, bone, and brain. At 60 min, the accumulation of ^{18}F-FBMHA in the liver was significantly greater ($P < 0.01$) than that in any of the other tissues sampled.

TABLE 2
Heart-to-Tissue Ratios for ^{18}F-FCPHA and ^{18}F-FBMHA

Ratio	Value for the following tracers at the indicated time:			
	^{18}F-FCPHA		^{18}F-FBMHA	
	5 min	60 min	5 min	60 min
Heart-to-lung	3.3	4.6	2.0	2.9
Heart-to-blood	25.8	20.4	2.6	2.9
Heart-to-muscle	6.2	14.3	3.9	4.1
Heart-to-liver	1.6	1.6	0.3	0.4

TABLE 3
Tissue Distribution of ^{18}F-FBMHA in Sprague–Dawley Rats

Tissue	Mean ± SD %ID/g at:	
	5 min	60 min
Blood	1.02 ± 0.22	0.58 ± 0.27*
Heart	2.56 ± 0.76	1.69 ± 0.13*
Lungs	1.25 ± 0.18	0.58 ± 0.17†
Liver	8.88 ± 2.97	4.17 ± 1.49*
Kidneys	2.62 ± 0.86	1.66 ± 0.61
Skeletal muscle	0.66 ± 0.22	0.41 ± 0.10
Bone	0.52 ± 0.16	2.36 ± 0.78†
Brain	0.25 ± 0.07	0.27 ± 0.03

*$P < 0.05$.
†$P < 0.01$.

The accumulation of ^{18}F-FBMHA in the heart was 2.56 ± 0.76 %ID/g at 5 min after injection and decreased to 1.69 ± 0.13 %ID/g at 60 min ($P < 0.05$). Nearly equal concentrations of radioactivity were detected in the heart and the kidneys at both times. Tracer activity in the blood at 5 min was 1.02 ± 0.22 %ID/g and decreased only to 0.58 ± 0.27 %ID/g at 60 min ($P < 0.05$). Most of the radioactivity accumulated in the liver (8.88 ± 2.97 %ID/g at 5 min vs. 4.17 ± 1.49 %ID/g at 60 min; $P < 0.05$). The heart-to-blood ratio of 2.6 at 5 min did not change significantly at 60 min (Table 2). Tracer accumulation in bone was 0.52 ± 0.16 %ID/g at 5 min and increased to 2.36 ± 0.78 %ID/g at 60 min ($P < 0.01$), indicating that there was significant defluorination. The biodistribution of ^{18}F-FBMHA in rats was analyzed again with a 4% Tween 80:saline formulation, and similar results were obtained (data not shown).

MicroPET Imaging

Representative transaxial PET images of the heart of a monkey were acquired at 60 min after administration of 6 mCi of ^{18}F-FCPHA and are shown in Figure 1. The corresponding time–activity curves for ROIs drawn over the left ventricular wall and cardiac blood pool are shown in Figure 2. The images clearly demonstrate a high level of tracer accumulation in the heart, with excellent definition of the left ventricle from the lungs and blood pool. The left ventricular time–activity curve shows rapid accumulation of the tracer. A plateau was achieved by approximately 10 min after injection and was maintained for the remainder of the study. The early transient increase in radioactivity was most likely attributable to blood flow. The blood time–activity curve shows an immediate increase in radioactivity followed by a rapid decline. The secondary slow increase in

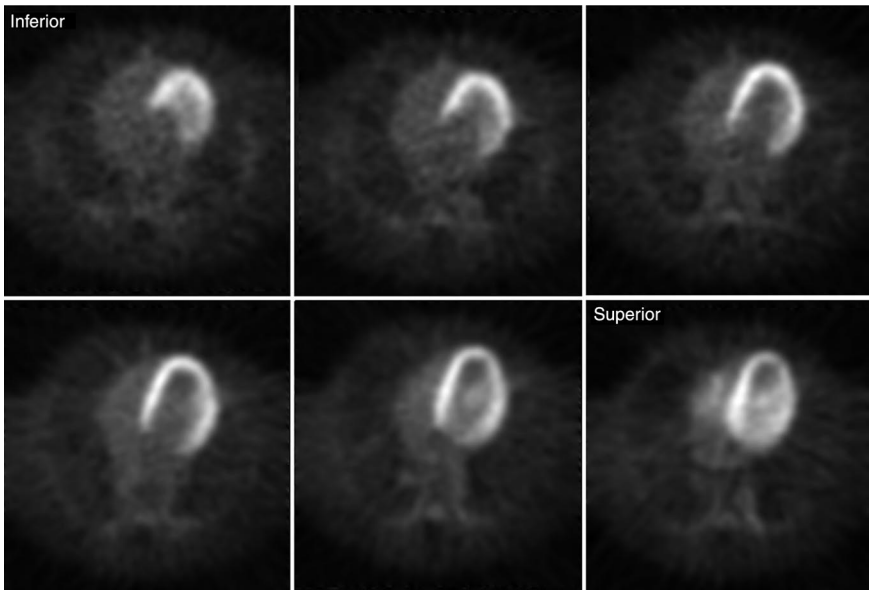

FIGURE 1. Transaxial heart-level slices acquired in rhesus monkey by use of positron camera (microPET model P4) 60 min after intravenous administration of 222 MBq of ^{18}F-FCPHA.

blood radioactivity most likely represented the release of radiolabeled metabolic products from the liver.

DISCUSSION

The myocardium can use lactate, acetate, fatty acids, and glucose to satisfy its contractile needs. Under aerobic circumstances, most of the energy for adenosine triphosphate production is provided by the complete oxidation of fatty acids (those containing between 14 and 18 carbons) to carbon dioxide and water. These products of catabolism are diffusible and are carried away from the myocytes as they are produced when blood flow is adequate. When blood flow is significantly reduced, tissue delivery of oxygen and removal of waste products are reduced. As a result, oxygen-dependent substrate catabolism decreases. Because fatty acids are catabolized by β-oxidation to acetyl coenzyme A (acetyl-CoA), which requires the Krebs cycle and ultimately oxidative phosphorylation to produce adenosine triphosphate, fatty acid consumption decreases with anoxia (i.e., zones of myocardial ischemia or infarction) (*25*).

Fatty acids pass from capillary blood into the interstitial space, where they may "back diffuse" to the vascular space or continue forward, passing through the sarcolemmal barrier. Once inside the cell, fatty acids may return to the interstitial space or become activated as acyl-CoA. Activated fatty acids then can be esterified to form triglycerides, incorporated into phospholipids, or carried into the mitochondria and oxidized. The activation of free fatty acids to acyl-CoA requires energy and is believed to be essentially irreversible in vivo. However, the formation of triglycerides is not irreversible, and these can be broken down into the constituent fatty acids and glycerol, adding to the free fatty

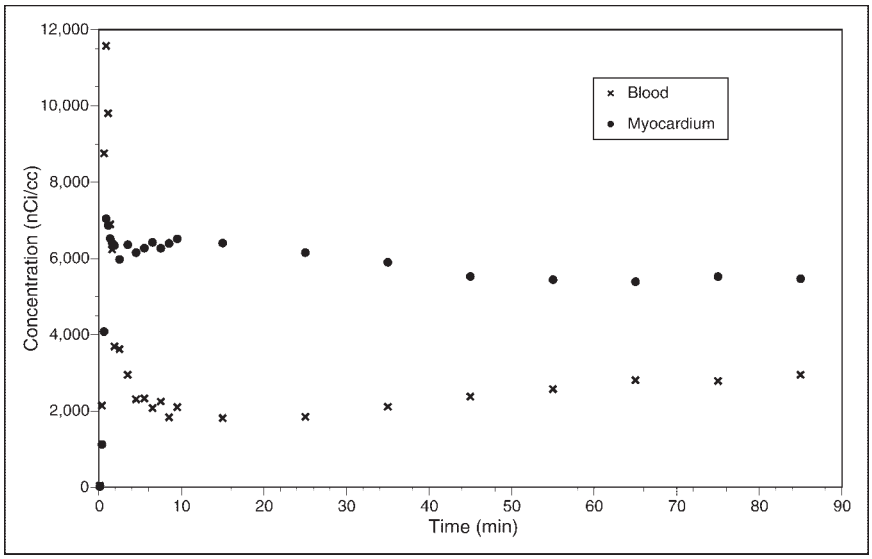

FIGURE 2. Time–activity curves for ROIs drawn over left ventricular wall and cardiac blood pool of rhesus monkey injected with 222 MBq of ^{18}F-FCPHA.

acid pool. Fatty acid β-oxidation occurs in the mitochondrial matrix, and fatty acids are actively transported from the cytoplasm into the mitochondria by carnitine palmitoyl transferase. The β-oxidation metabolic process involves 4 reactions that occur in repeating cycles (Fig. 3). In each cycle, a fatty acid is progressively shortened by 2 carbons as it is oxidized and its energy is captured by the reduced energy carriers reduced nicotinamide adenine dinucleotide and reduced flavin adenine dinucleotide (*26*). At the end of each cycle, acetyl-CoA is released and either returns to the cytoplasm and is used in various synthetic reactions or enters the Krebs cycle to produce carbon dioxide and water. The oxidative process is repeated for various numbers of cycles until the fatty acid is entirely converted to acetyl-CoA (even carbon chain) or propionyl-CoA (odd carbon chain). β-Oxidation requires less than 2 min to complete the catabolism of a typical 16-carbon fatty acid, such as palmitate.

To obtain measurements of fatty acid metabolism with high precision, it is important to use a fatty acid analog that, like ^{18}F-FDG, enters the metabolic pathway but is retained in the tissues for a prolonged period of time. Such an analog would mirror the initial uptake characteristics of palmitate, proceed through the steps of activation to acyl-CoA, enter the mitochondria, and proceed though several steps of the catabolic cycle before being trapped in the cell. Previously, Livni et al. (*19*) and Elmaleh et al. (*20*) designed ^{11}C-BMHA, a branched-chain fatty acid with a methyl group placed at position 3 to inhibit β-oxidation by precluding the formation of the keto-acyl-CoA intermediate (step 3 in Fig. 3). When ^{11}C-BMHA was compared with ^{14}C-palmitate, similar myocardial uptake of the 2 agents was noted; however, there was prolonged retention of ^{11}C-BMHA, which cannot undergo β-oxidation, and hence it is either trapped in the mitochondria or incorporated into the triglyceride pool. The concentration of ^{11}C-BMHA in myocardial tissue after intravenous injection reaches a plateau after 10–15 min. Because the triglyceride pool turns over very slowly, as indicated by measurements with palmitate, the plateau of activity represents both uptake and pool components.

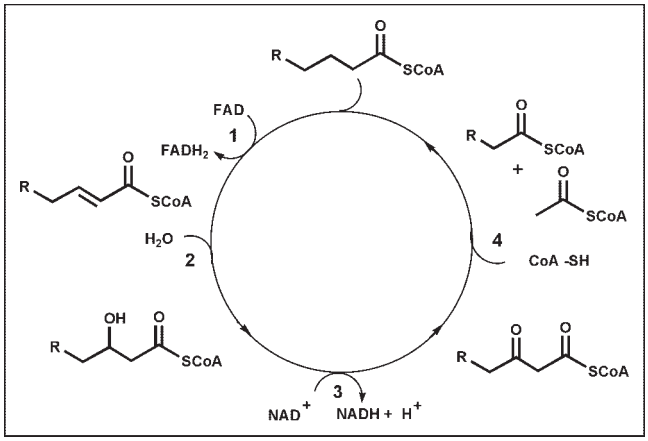

FIGURE 3. Metabolic pathway for β-oxidation. Each cycle involves 4 reactions: 1, acyl-CoA dehydrogenase; 2, enoyl-CoA hydratase; 3, 3-hydroxyacyl-CoA dehydrogenase; and 4, β-keto-acyl-CoA thiolase. FAD = flavin adenine dinucleotide; $FADH_2$ = reduced flavin adenine dinucleotide.

^{18}F-labeled 3-methyl- and 5-methyl-substituted 16-fluoropalmitic acid analogs have been prepared, and their evaluation in rats showed lower uptake but longer retention of radioactivity in the myocardium compared with those of 16-^{18}F-fluoropalmitate (*27–29*). There was also high uptake of radioactivity in bone, an indication of defluorination. ω-Oxidation of fatty acids, albeit a minor metabolic pathway, occurs in the endoplasmic reticulum rather than the mitochondria and may account for the instability of these ω-labeled analogs.

Another PET tracer, 14-^{18}F-fluoro-6-thiaheptadecanoic acid (FTHA), has been proposed as a probe for myocardial oxidative metabolism (*30*). FTHA is a "false" long-chain fatty acid substrate in which a sulfur atom has been inserted at position 6 to block complete catabolism. Evaluation of FTHA has shown high myocardial uptake in animals and humans, with a heart-to-blood ratio similar to that of a blood flow agent. The biodistribution of FTHA in mice showed a large amount of activity in bone, indicating defluorination. Our work, in collaboration with that of Okada et al. (*31*), who evaluated tellurium as a heteroatom in the fatty acid backbone, revealed high myocardial uptake similar to that of FTHA in animals. Although FTHA has promise as a myocardial imaging agent, we prefer the use of a fatty acid with an all-carbon backbone, a more natural fatty acid structure, because of potential complications of image interpretation. The biologic behavior of these natural molecules and the identification of their metabolites have been completely determined. Therefore, we compared our recent results with results obtained with fatty acid probes that have similar all-carbon backbones.

Cyclopropane fatty acids occur in a variety of plants and animals but most prominently in bacterial phospholipids (*32*). The discovery of lactobacillic acid, *cis*-11,12-methyleneoctadecanoic acid, led to considerable interest in the metabolism and function of cyclopropane fatty acids (*33*). Its 17-carbon analog, *cis*-9,10-methylenehexadecanoic acid, was shown to be present in phospholipids of bovine heart (about 4% of all fatty acids) and liver mitochondria (*34*). It has also been reported that *cis*-3,4-methylenehexanedioic acid is present in human urine and that it is a metabolite of *cis*-9,10-methylenehexadecanoic acid; however, the origin and physiologic role of these compounds remain unclear (*35*). Interestingly, experiments have shown that *cis*-9,10-methylenehexadecanoic acid and its 18-carbon analog cannot be metabolized beyond a certain length in rat liver mitochondria. Data suggest that β-oxidation occurs until the cyclopropyl moiety is reached, because 3,4-methylenedecanoic and 3,4-methylenedodecanic acids have been found as metabolic products (*36*).

In our study, ^{18}F-FCPHA showed fast blood clearance and excellent heart uptake and retention. Its heart-to-blood

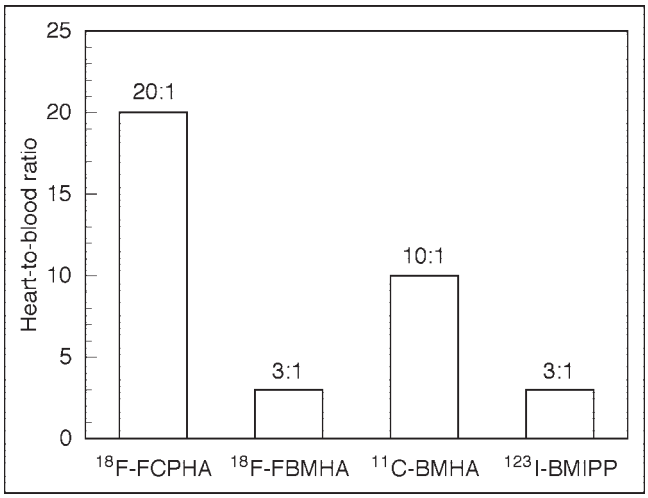

FIGURE 4. Summary of heart-to-blood ratios of modified fatty acids at 60 min after intravenous injection.

ratio of 20:1 in rats at 60 min is significantly higher than those of BMHA (10:1) and BMIPP (3:1) (Fig. 4). PET imaging of the monkey heart after injection of ^{18}F-FCPHA exhibited an initial spike of activity corresponding to blood flow followed within 10 min by a plateau that remained constant for over 1 h. In contrast, compared to ^{18}F-FCPHA, the β-methyl analog ^{18}F-FMBHA showed slower blood clearance along with a greater accumulation of activity in the liver and bone. The heart-to-blood ratio obtained with ^{18}F-BMHA was 2.6 at 5 min and did not change significantly at 60 min, indicating the retention of activity. These results clearly illustrate the unique influence of the cyclopropyl moiety on the manner in which ^{18}F-FMBHA accumulates in the heart. The high liver and bone uptake of the β-methyl analog may be associated with its inability to be irreversibly trapped in the myocardium, because ^{18}F-FBMHA and ^{11}C-BMHA should have the same uptake mechanisms. Like ^{11}C-BMHA, ^{18}F-FBMHA may experience back diffusion before it is incorporated into the cytosolic lipid pool and mitochondria, events that may increase the chance of defluorination. A comparative study of ^{11}C-BMHA and ^{11}C-CPHA would be useful to evaluate the direct effect of the cyclopropyl moiety on heart uptake.

The mechanism for ^{18}F-FCPHA uptake in the myocardium may center on the irreversible formation of the cyclopropanol derivative produced in step 2 of the β-oxidation cycle, because cyclopropanols are unstable and are known to undergo rearrangement under mild conditions (*37*). Alternatively, ^{18}F-FCPHA accumulation may be the result of an interaction between the cyclopropyl moiety and the enzymes associated with the β-oxidation process. It is known that the active metabolite methylenecyclopropylacetyl-CoA (MCPA-CoA), produced from the degradation of hypoglycin A, accumulates in rat liver mitochondria (*38*). The mechanism of this effect is believed to be an irreversible inhibition of β-oxidation that results from the reaction of MCPA-CoA with the flavin of general acyl-CoA dehydrogenase. The same methylenecyclopropyl moiety found in MCPA-CoA is theoretically produced when ^{18}F-FCPHA-SCoA enters the β-oxidation cycle and undergoes dehydrogenation via acyl-CoA dehydrogenase (step 1 of the oxidation cycle). In this form, the cyclopropane moiety, by virtue of its ring strain and electron-withdrawing substituent, may be readily susceptible to nucleophilic attack, thus trapping the tracer in the mitochondria (Scheme 2). A similar mechanism has been proposed for several cyclopropane-containing compounds; in this mechanism, an enzyme activates the cyclopropane ring for nucleophilic addition by the oxidation or protonation of the adjacent group, rendering the substituent more capable of electron withdrawal (*39*).

CONCLUSION

The results of this study suggest that the cyclopropyl moiety in ^{18}F-FCPHA is responsible for the unusually high heart uptake and fast blood clearance for this tracer. The high heart-to-blood ratio and excellent images obtained with ^{18}F-FCPHA indicate the potential of this class of compounds for evaluating myocardial fatty acid metabolism by PET. The preliminary data obtained with ^{18}F-FCPHA warrant additional pharmacokinetic and metabolic fate investigations to further evaluate its in vivo behavior and establish logical hypotheses for designing future analogs.

REFERENCES

1. Okada RD, Boucher CA, Strauss HW, et al. Exercise radionuclide imaging approaches to coronary artery disease. *Am J Cardiol*. 1980;46:1188–1204.
2. Pohost GM, Alpert NM, Ingwall JS, et al. Thallium redistribution: mechanism and clinical utility. *Semin Nucl Med*. 1980;11:70–93.
3. Heyndrickx GR, Millard RW, McRitchie RJ, et al. Regional ventricular function and electrophysiological alterations after brief coronary occlusion in conscious dogs. *J Clin Invest*. 1975;56:978–985.
4. Braunwald E, Kloner RA. The stunned myocardium: prolonged postischemic ventricular dysfunction. *Circulation*. 1982;66:1146–1149.

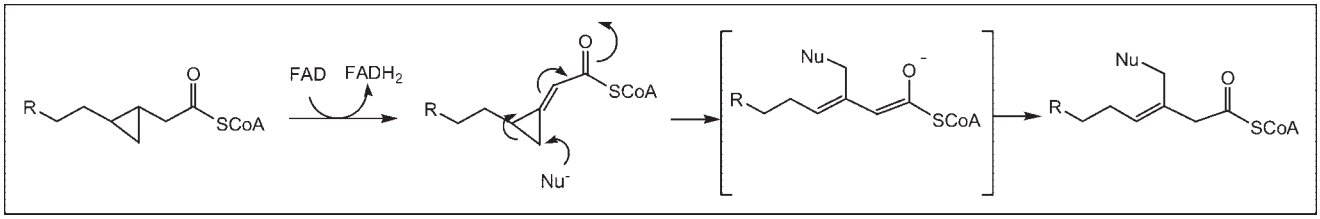

SCHEME 2. Possible trapping mechanism for ^{18}F-FCPHA in mitochondria. FAD = flavin adenine dinucleotide; $FADH_2$ = reduced flavin adenine dinucleotide. Nu^- = nucleophile.

5. Greenberg JM, Murphy JH, Okada RD, et al. Value and limitations of radionuclide angiography in determining the cause of reduced left ventricular ejection fraction: comparison of idiopathic dilated cardiomyopathy and coronary artery disease. *Am J Cardiol*. 1985;55:541–544.
6. Kaul S, Boucher CA, Newell JB, et al. Determination of the quantitative thallium imaging variables that optimize detection of coronary artery disease. *J Am Coll Cardiol*. 1986;7:527–537.
7. Phelps ME, Hoffman EJ, Selin C, et al. Investigation of [^{18}F]2-fluoro-2-deoxyglucose for the measure of myocardial glucose metabolism. *J Nucl Med*. 1978; 19:1311–1319.
8. Ratib O, Phelps ME, Huang SC, Henze E, Selin CE, Schelbert HR. Positron tomography with deoxyglucose for estimating local myocardial glucose metabolism. *J Nucl Med*. 1982;23:577–586.
9. Liu P, Kiess MC, Okada RD, et al. The persistent defect on exercise thallium imaging and its fate after myocardial revascularization: does it represent scar or ischemia? *Am Heart J*. 1985;110:996–1001.
10. Rocco TP, Dilsizian V, McKusick KA, Fischman AJ, Boucher CA, Strauss HW. Comparison of thallium redistribution with rest reinjection imaging for the detection of myocardial ischemia. *Am J Cardiol*. 1990;66:158–163.
11. Jadvar H, Strauss HW, Segall GM. SPECT and PET in the evaluation of coronary artery disease. *RadioGraphics*. 1999;19:915–926.
12. Bergmann SR. Use and limitations of metabolic tracers labeled with positron-emitting radionuclides in the identification of viable myocardium. *J Nucl Med*. 1994;35(suppl):15S–22S.
13. Grandin C, Wijns W, Melin JA, et al. Delineation of myocardial viability with PET. *J Nucl Med*. 1995;36:1543–1552.
14. Most AS, Brachfield N, Gorlin R, Wahren J. Free fatty acid metabolism of the human heart at rest. *J Clin Invest*. 1969;48:1177–1188.
15. Tamaki N, Morita K, Kuge Y, Tsukamoto E. The role of fatty acids in cardiac imaging. *J Nucl Med*. 2000;41:1525–1534.
16. Klein MS, Goldstein RA, Welch MJ, Sobel BE. External assessment of myocardial metabolism with [^{11}C]palmitate in rabbit hearts. *Am J Physiol*. 1979;237: H51–H58.
17. Goldstein RA, Klein MS, Welch MJ, Sobel BE. External assessment of myocardial metabolism with C-11 palmitate in vivo. *J Nucl Med*. 1980;21:342–348.
18. Bergmann SR, Weinheimer CJ, Markham J, Herrero P. Quantitation of myocardial fatty acid metabolism using PET. *J Nucl Med*. 1996;37:1723–1730.
19. Livni E, Elmaleh DR, Levy S, Brownell GL, Strauss WH. Beta-methyl[1-^{11}C]heptadecanoic acid: a new myocardial metabolic tracer for positron emission tomography. *J Nucl Med*. 1982;23:169–175.
20. Elmaleh DR, Livni E, Levy S, Varnum DA, Strauss HW, Brownell GL. Comparison of ^{11}C- and ^{14}C-labeled fatty acids and their beta-methyl analogs. *Int J Nucl Med Biol*. 1983;10:181–187.
21. Elmaleh DR, Livni E, Alpert NM, Strauss HW, Buxton R, Fischman AJ. Myocardial extraction of 1-[^{11}C] betamethylheptadecanoic acid. *J Nucl Med*. 1994;35:496–503.
22. Livni E, Elmaleh DR, Barlai-Kovach MM, et al. Radioiodinated beta-methyl phenyl fatty acids as potential tracers for myocardial imaging and metabolism. *Eur Heart J*. 1985;6:85–89.
23. Knapp FF Jr. Myocardial metabolism of radioiodinated BMIPP. *J Nucl Med*. 1995;36:1051–1054.
24. Faust F. Fascinating natural and artificial cyclopropane architectures. *Angew Chem Int Ed*. 2001;40:2251–2252.
25. Opie LH. Effects of regional ischemia on metabolism of glucose and fatty acids. *Circ Res Suppl*. 1976;38:52–77.
26. Luiken J, Schaap FG, Nieuwenhoven FA, et al. Cellular fatty acid transport in heart and skeletal muscle as facilitated by proteins. *Lipids*. 1999;34(suppl):S169–S175.
27. Livni L, Elmaleh DR. Synthesis of 16-[^{18}F]fluorobetamethylhexadecanoic acid and 16-[^{18}F]fluorohexadecanoic acid. In: Vaalburg W, ed. *7th International Symposium on Radiopharmaceutical Chemistry*. Groningen, The Netherlands: University of Groningen; 1988:231–232.
28. Goodman MM, Knapp FF. Radiochemical synthesis of [^{18}F]-3-methyl-branched omega fluoro-fatty acids. In: Vaalburg W, ed. *7th International Symposium on Radiopharmaceutical Chemistry*. Groningen, The Netherlands: University of Groningen; 1988:233–235.
29. Nishimura S, Takahashi T, Ido T, Ishiwata K, Iwata R. Development of branched-chain ^{18}F-fluoro-fatty acids for evaluating regional beta-oxidation in the heart [abstract]. *J Nucl Med*. 1990;31(suppl):901P.
30. DeGrado TR, Coenen HH, Stöcklin G. 14(*R,S*)-[^{18}F]Fluoro-6-thia-heptadecanoic acid (FTHA): evaluation in mouse of a new probe of myocardial utilization of long chain fatty acids. *J Nucl Med*. 1991;32:1888–1896.
31. Okada R, Knapp FF, Elmaleh DR, et al. Tellurium-123m labeled 9-telluraheptadecanoic acid: a possible cardiac imaging agent. *Circulation*. 1982;65:305–310.
32. Yano I, Nichols BW, Morris LJ, James AT. The distribution of cyclopropane and cyclopropane fatty acids in higher plants. *Lipids*. 1972;7:30–34.
33. Hofman K Luca RA, Sax SM. The chemical nature of the fatty acid of *Lactobacillus arabinosus*. *J Biol Chem*. 1951;195:473–485.
34. Sakurada K, Iwase H, Takatori T, et al. Identification of *cis*-9,10-methylenehexadecanoic acid in submitochondrial particles of bovine heart. *Biochim Biophys Acta*. 1999;1437:214–222.
35. Greter J, Lindstedt S, Steen G. Urinary metabolites of *cis*-9,10-methylenehexadecanoic acid. *J Biol Chem*. 1979;254:2807–2813.
36. Chung AE. Metabolism of cyclopropane fatty acids oxidation of *cis*-9,10-methylene hexadecanoic and *cis*-9,10-methylene octadecanoic acids by rat-liver mitochondria. *Biochim Biophys Acta*. 1966;116:205–213.
37. DePuy CH. The chemistry of cyclopropanols. *Accounts Chem Res*. 1968;1:33–41.
38. Mellde K, Jackson S, Bartlett K, et al. Metabolic consequences of methylenecyclopropyl glycine poisoning in rats. *Biochem J*. 1991;274:395–400.
39. Li D, Agnihotri G, Dakoji S, Oh E, Lantz M, Liu H. The toxicity of methylenecyclopropyl glycine. *J Am Chem Soc*. 1999;121:9034–9042.